Al-Qadisiyah Journal for Engineering Sciences 16 (2023) 239–246

Contents lists available at http://qu.edu.iq

Al-Qadisiyah Journal for Engineering Sciences

Journal homepage: https://qjes.qu.edu.iq

Develop a new mathematical approach to predict the crack propagation rate in a thin plate subjected to in-plane biaxial loading

Israa Abed Alrazak Mosleh and Fathi A. A. Alshamma

Deparment of mechincal Enginering, College of Engineering, Baghdad University, Iraq

ARTICLE INFO

Article history:
Received 10 May 2023
Received in revised form 28 August 2023
Accepted 01 November 2023

Keywords:
Combined loads
Crack propagation
Cycling shear stress
Edge crack
Propagation

ABSTRACT

The mechanical design of metals must deal with structures collapsing due to cracks occur in the material. This study focused on the edge crack at non-proportional cycle loading because it propagates quickly. This research attempted to determine two mathematical models that could predict the crack propagation rate for thin samples of aluminum alloy types 6061 and 5052 under constant tensile stresses and cyclic shear stress applied within the elastic limits of the material using "Griffith energy of dynamic fracture". This was performed to evaluate if these models can predict crack growth rates and compare with the numerical results of a computer system in the ANSYS program R1 2021. The direction of the crack path was calculated and compared with the analytical program. The results of the two mathematical models in predicting the dynamic growth rate in the studied alloys gave low error rates to the numerical solution.

1. Introduction

When the value of the stress intensity factor for the material (K_I) reaches the critical value as a result of the stress that is applied to it, then the crack starts to grow gradually, passing the first stage of all three stages of spreading a crack, which is the stage of not growing in it because the "intensity stress factor equivalent (K_{eq})" value is less than the intensity stress factor endurance (K_{th}) value according to the Eq. 1 [1]. It is important to note that mechanical fracture in a structure occurs due to the presence of cracks. The second stage is when the crack develops in a stable state, which is characterized as occurring when the value of the intensity stress factor equivalent (k_{eq}) reaches or is greater than the allowable limit. This stage occurs when the fracture is stable. This step is symbolized by the Paris equation [2-3], which may be written as follows, Eq. 1.

$$\frac{da}{dN} = C(\Delta k_{equ})^m \quad (1)$$

Where C and m constant factors are discovered empirically, (da/dN) is the ratio of the difference in crack length to the difference in number of cycles, and it is a linear stage in which the length of the crack grows with the increase in the number of cycles. The last stage, which is the stage of instability in the formation of the fracture, is one in which the growth is fast and collapse takes place while it is taking place. Many studies are being conducted in an effort to understand and find a treatment for the propagation of cracks in materials, such as spot welding. Al.Shamma and Ahmed investigated the influence of crack formation as well as the study of raising the stress ratio on a thin plate by increasing the number of rotations. This was done using an impact load [4].

* *Corresponding author.*
E-mail address: israa.mosleh2003m@coeng.uobaghdad.edu.iq (Israa. Mosleh)

https://doi.org/10.30772/qjes. 2023.142855.1023

Nomenclature:

K_{eq}	stress intensity factor equivalent ((MPa$\sqrt{m}$)	m	mass of the material (K.g)
K_{th}	stress intensity factor endurance ((MPa$\sqrt{m}$)	T_{total}	total amount of kinetic energy (Joule)
m	constant factor of Paris equation, unit less.	G	the additional amount of release energy (Joule)
C	constant factor of Paris equation, (mm/cycle) / (MPa$\sqrt{m}$).	R	represents the amount of energy that is being resisted by the fracture (Joule)
a	length of crack (m)	K_I	stress intensity factor for mode I, MPa$\sqrt{m}$.
a_i	the last length in the crack (m)	K_{II}	stress intensity factor for mode II, MPa$\sqrt{m}$.
a_o	the original length of the crack's length (m)	σ_{eff}	The effective stress for the mixed mode (MPa)
E’	modulus of elastic (MPa)	U	The total amount of excess energy (Joule)
v	displacement for the Mode-I.	U_O	the amount of excess energy per unit of thickness (Joule)
u	displacement for the Mode-II	da /dt	rate of crack growth (m/sec)
V	displacement for the mixed mode (I/II).	*Greek symbols*	
$\dot{v}$	the rate of displacement for the Mode I .	Θ_c	Angel of crack, Degree
$\dot{u}$	the rate of displacement for the Mode II.	ϕ_{ZI}	Stress function for first mode
$\dot{V}$	the rate of displacement for the mixed mode (I/II).	ϕ_{ZII}	Stress function for second mode
τ_o	max value of shear stress (MPa)	σ	tension stress (MPa)
τ	shear cycling load (Mode-II) (MPa)	*Subscripts*	
w	angular velocity, (rad /sec).	eff	effective
t	time (Sec)	c	critical
		equ	equivalent

Jasim investigated a number of different kinds of epoxy coatings that have the potential to enhance the resistance of the material to the occurrence of dynamic crack propagation and to raise the resistance of the material to fracture. These epoxy coatings have the potential to be employed to cover water tanks [5]. Kopei Made the suggestion that liquid be added to the inside of the rods that back up huge pumps in order to strengthen their resistance to secondary cracks and fractures [6]. Al- Jaafari subjected a variety of aluminium alloys to thermal treatment and investigated the impact that this modification had on the redistribution of nanoparticles that occurred as a consequence of the treatment on the dynamic crack formation condition when the number of cycles was increased [7]. Ibrahim Mhuwes conducted research to determine the amount of fracture propagation in plates of varying thicknesses and at an assortment of angles [8]. But these treatments are just temporary solutions; the best method to fix the problem is to enhance the technical design and make sure there are no fractures in the machine or the mechanical structure. For this reason, it is required to make a prediction about the time of occurrence of the crack as well as its rate of spread in order to stop its propagation. Additionally, it is necessary to locate a suitable mathematical model that is capable of giving results that are comparable to the development of the crack and its behaviour in real life. The equations that were generated were used on two different series of aluminium alloys [9-10], type 6061 and type 5052, at the “UNI-standard system**”** at room conditions (Humidity of 20% and Temperature of 27 C). Where the dimensions of the sample 160 X 40 mm with a thick 2 mm and length edge crack is 5 mm.

The main objectives of this study are as follows:

- Development of two unlike mathematical models that are capable of predicting the percentage of crack propagation in the edge for the two alloys.
- Looking for the optimal derivative calculation model that will provide findings that are as close as possible to those produced by the computer analysis software in terms of predicting how the crack will behave in the material.

2. Method

2.1. Theoretical Analysis

It is quite difficult to come up with an analytical model that can accurately forecast the ratio of dynamic crack propagation and have its findings correspond with the actual values that are obtained for the material in real life. This is due to the fact that developing such a model requires a lot of time and effort. The following assumptions have been worked on to get the equations for thin plates that have been subjected to tension load and shear cyclic loading under an applied mixed cycling load. Therefore, this research endeavoured to come as close as possible to the practical results that had been obtained by working on two mathematical formulas using "Griffith's theory of energy" within a "Linear Elastic Fracture Mechanical LEFM". The assumptions that were used to derive the equation were as follows:

- Hooke's law is followed by the material, which shows linear elasticity.
- It has the properties of being isotropic and homogenous.
- The cycling stress occurs along axes that are perpendicular to the load that is being tensioned.
- Shear stress cycling is applied in the plane.
- A sample is a thin plate with edge crack.

2.1.1. First theoretical approach (separation of modes)

Since most of the research was concerned with the study of cracks, it was found that the "Westergaard equation was used in many cases of cracks occurring in the material. In this research, it was used in Mode-I and Mode-II by derived two mathematical models; the main equation of Westergaard was relied upon. The resultant outcomes will then be compared with the numerical solution values.

Apply the “Westergaard's stress function” in order to analyse fracture propagation in the Mode-I [10].

$$\phi_{ZI} = \frac{\sigma \cdot Z}{\sqrt{Z^2 - a^2}} \quad (2)$$

The following relations are derived from Fig. 1, which is as follows [11]:

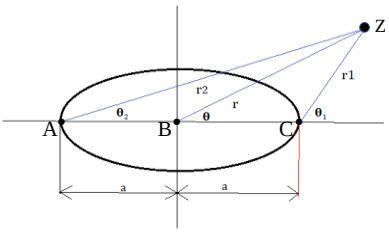

Figure 1. Theory of cracks that show the complex variable functions [10]

When the complex variable Z gives a complex root for a point located on the plate, this point is defined with respect to three points on the plate, namely A, B, and C, as following Eqs. (3-5):

$$Z = r \,.\, e^{\,i\boldsymbol{\theta}} \tag{3}$$

$$Z - a = r_1 \,.e^{\,i\boldsymbol{\theta}_1} \tag{4}$$

And

$$Z + a = r_2 .\, e^{\,i\boldsymbol{\theta}_2} \tag{5}$$

According to the (Eqs. 2-5) have the potential to attain the displacement (v) for the Mode-I [13-14]will be as following:

For plain strain :

$$v = \frac{2\sigma}{E}(1-\upsilon^2).\sqrt{a^2-x^2}$$

For plain stress:

$$\mathrm{v} = \frac{2\sigma}{\mathrm{E}'}.\sqrt{\mathrm{a}^2-\mathrm{x}^2} \tag{6}$$

Where $(1/\mathrm{E}`) = (1-\upsilon^2)/\mathrm{E}$, and v is represented the displacement that result due to tensile load.

Assume $x = c.a \quad (0 < x < 1)$, let $c_1 = 2\sqrt{1-c^2}$, use (Eq.6) in the equation to find displacement v, as shown in Fig .2.

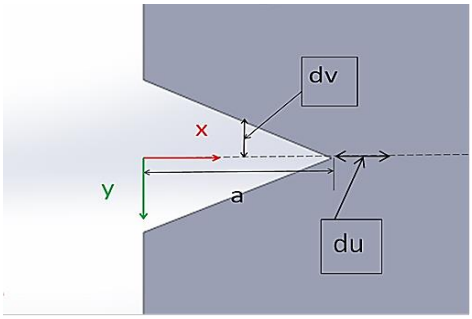

Figure 2. The displacements v and u

$$\mathrm{v} = \frac{c_1 .\sigma.a}{\mathrm{E}} \tag{7}$$

According to the reference of the Fracture Mechanics book [10] for the Elastic Stress Field Displacement (v) as shown in Fig. 2, is that the crack flank field displacement where the coordinate system for X and Y at the beginning of the notch and for Mode-II is based on the fundamentals of Fracture Mechanics book [14]

The following is a description of the stress function for In-plane shear stress in the Mode–II (ϕZ_{II}), which is denoted by:

$$\phi \mathrm{Z_{II}} = \frac{\tau \,.\, z}{\sqrt{(z^2-a^2)}} \tag{8}$$

According to the source [14], the displacement at the cycle shear stress (u) for Mode-II is the outcome of doing an integral [15].

$$\bar{\mathrm{Z}}_{\mathrm{II}} = \tau.\sqrt{z^2-a^2} \tag{9}$$

$z = x + iy \ldots\ldots\ldots at\ y = 0, z = x \ \ \& \ \ x \ll a$, will result [14], [16]:

For plane strain

$$\mathrm{u} = \frac{2(1-\upsilon^2)}{\mathrm{E}} .\tau\sqrt{\mathrm{a}^2-\mathrm{x}^2}.$$

For plain stress

$$\mathrm{u} = \frac{2}{\mathrm{E}'} .\tau\sqrt{\mathrm{a}^2-\mathrm{x}^2} \tag{10}$$

It is started by measuring the horizontal and vertical displacements at the same location, which is at the beginning of the notch, but the effect of the displacement u appears when the two surfaces of the crack meet, when it is assumed that the sample is homogeneous and without deformation occurring while it is exposed to loads.

Where (u) the displacement for the shear cycling load (Mode-II) and value of shear stress cycling ($\boldsymbol{\tau} = \boldsymbol{\tau}_o \,.\, \sin\left(\frac{\mathrm{wt}}{2}\right)$)[17], as shown in Fig. 3, found the rate of displacement $\dot{\boldsymbol{\upsilon}}$ and $\dot{\mathrm{u}}$ by derivate the (Eq. 7) and (Eq. 10)

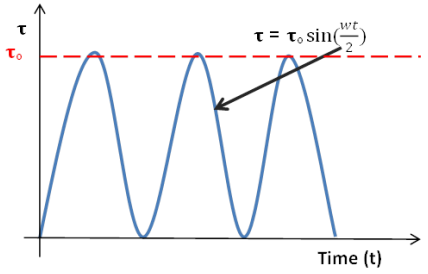

Figure 3. Shear cycling stress

$$\dot{\mathrm{v}} = \frac{c_1 .\sigma\dot{\mathrm{a}}}{\mathrm{E}`} \tag{11}$$

Where $\dot{\mathrm{v}}$ is represented the rate of the displacement that result due to tensile load (v) (where the displacement v will change with time and for denoting this rate of change d/dt represented by "•"and in this case the change is happening in displacement(v) with length of the crack(a)).

$$\dot{\mathrm{u}} = \frac{c_1}{\mathrm{E}}\left[\mathrm{a}.\frac{\mathrm{w}}{2}.\tau_o.\cos\left(\frac{\mathrm{wt}}{2}\right) + \tau_o.\sin\left(\frac{\mathrm{wt}}{2}\right).\frac{\mathrm{da}}{\mathrm{dt}}\right] \tag{12}$$

While u̇ is represented the rate of the displacement that result due to shear cycling load (u) (where the displacement u will change with time and for denoting this rate of change d/dt represented by "•"and in this case the change is happening in displacement (u) with length of the crack(a) and change in the rate of the shear cycling load ($\boldsymbol{\tau}_o . \sin(\frac{wt}{2})$).
To find the total kinetic energy (T_{total}) [18] for Mixed-modes I/II. Since the kinetic energy per unite thickness for Mode-I and Mode-II are Non-directional quantities , it can be summed as follow:

$$T_{total} = \frac{1}{2}m\dot{v}^2 + \frac{1}{2}m\dot{u}^2 \quad (13)$$

$$= \frac{1}{2}.\rho.area.\dot{v}^2 + \frac{1}{2}.\rho.area.\dot{u}^2 \quad (14)$$

After substituting equations v and u, the following are the results of integrating the Equation:

$$T_{total} = \frac{\rho}{2E^2}.Ka_i^2[\left(\sigma^2 + {\tau_o}^2\sin^2\left(\frac{wt}{2}\right)\right)\left(\frac{da}{dt}\right)^2 + a_o.\frac{w}{2}.{\tau_o}^2.\sin(wt)\left(\frac{da}{dt}\right) + {\tau_o}^2 a_o^2.\frac{w^2}{4}.\cos^2\left(\frac{wt}{2}\right)] \quad (15)$$

To find the release energy rate (U) [19],[20], that is controlled on crack extension at the Mixed Modes (I / II) in thin plates [10], [21] for the Fig. 4 below,

$$U = \int_{a_o}^{a_i}(G - R).da = -\int_{a_o}^{a_i} R.da + \int_{a_o}^{a_i} G.da \quad (16)$$

The total excess energy is:

$$U_o = (\frac{\sigma^2}{2E} + \frac{2(1+v)}{E}\left(\tau_o.\sin\frac{wt}{2}\right)^2) \quad (17)$$

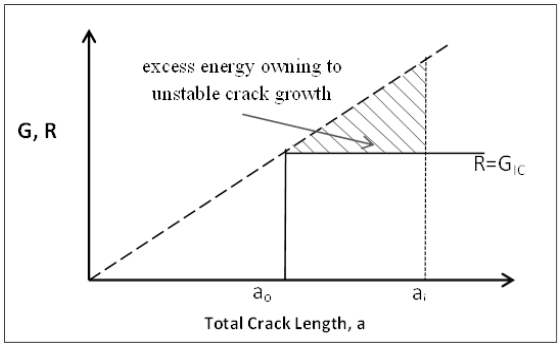

Figure. 4. Energy balance of the crack [10]

Physically, it has been scientifically proven in previous studies [11-23] that the deformation that appears at the crack edge, which forms the plastic area around and at the front of the crack, gives an enhancement to the resistance to the appearance of cracks, and therefore the necessary energy that the crack needs in order to start growing is higher in the crack at the middle because there are two tips of the crack in the center crack in the plate. Since noting that the excess energy to start the crack growing is less in the case of a crack at the edge, and since studies have shown that the energy circle surrounding the crack in the middle crack has a diameter of 2a, the assumption on which this research was based was used to be the diameter of the circle less and equal to a as shown in Fig. 5. The amount of excess energy rate per unit of thickness in edge crack as follows:

$$U = \left(\frac{\sigma^2}{2E} + \frac{2(1+v)}{E}\left(\tau_o.\sin\frac{wt}{2}\right)^2\right)\frac{\pi a^2}{4} \quad (18)$$

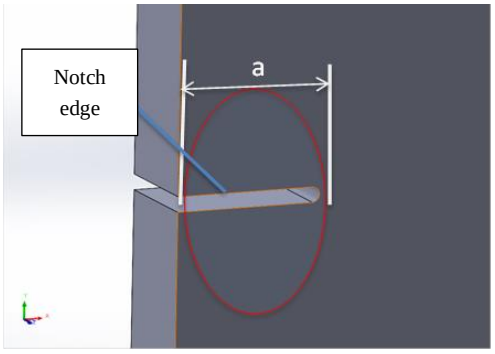

Figure 5. The area of energy in notch edge

When the fracture begins to spread, the value of the excess energy is converted into the total energy converts into kinetic energy and heat, where the heat energy is small in a thin plate and it can be neglected ($U = T_{total}$).

$$\left(\frac{\sigma^2}{2E} + \frac{2(1+v)}{E}\left(\tau_o.\sin\frac{wt}{2}\right)^2\right)\frac{\pi}{4}(a_i - a_o)^2 = \frac{\rho}{2E^2}.Ka_i^2[\left(\sigma^2 + {\tau_o}^2\sin^2\left(\frac{wt}{2}\right)\right)\left(\frac{da}{dt}\right)^2 + a_o.\frac{w}{2}.{\tau_o}^2.\sin(wt)\left(\frac{da}{dt}\right) + {\tau_o}^2 a_o^2.\frac{w^2}{4}.\cos^2\left(\frac{wt}{2}\right)] \quad (19)$$

When Eq. 19, is the number one model of the crack growth equation.

2.1. Second theoretical approach (mixed the modes)

In addition to this, the "Westergaard's stress function" [13] should be used in order to analyse crack propagation in Mixed-mode I/II [10]. For the purpose of determining the displacement (*V*) for the Mixed-mode I/II.

$$V = \frac{2\sigma_{eff}}{E'}\sqrt{a^2 - x^2} \text{ (plain stress)} \quad (20)$$

Assume $x = ca \quad 0 < x < 1$, let $c_1 = 2\sqrt{1 - c^2}$, Sub in the (Eq. 20)

$$V = \frac{c_1.\sigma_{eff}.a}{E'} \quad (21)$$

When the effective stress ($\boldsymbol{\sigma}_{eff}$) [23] for a combined mode that comes from tension load in the axis and cycling shear load in the elastic range in Pascal [21], as shown in Fig. 6, comes from the combination of tensile load and shear load cycling.

$$\sigma_{eff} = \frac{1}{\sqrt{2}}\sqrt{[\sigma^2 + (\tau_o.\sin\left(\frac{wt}{2}\right))^2]} \quad (22)$$

Determine the rate of displacement V by sub (Eq. 22) in (Eq. 21), then derive the equation for stress and crack length variables.

$$\dot{V} = \frac{c_1}{E}[\frac{a_o}{\sqrt{2}}.\frac{w.\tau_o^2.\sin(wt)}{4\left[\sigma^2 + \left(\tau_o.\sin\left(\frac{wt}{2}\right)\right)^2\right]^{1/2}} + \frac{1}{\sqrt{2}}\left[\sigma^2 + \left(\tau_o.\sin\left(\frac{wt}{2}\right)\right)^2\right]^{\frac{1}{2}}.\frac{da}{dt}] \quad (23)$$

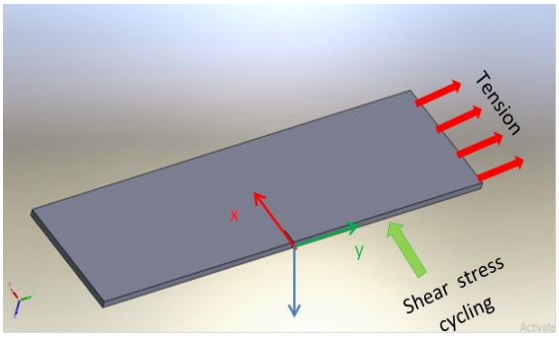

Figure 6. Loads on the sample

In order to calculate the total amount of kinetic energy (T_{total}):

$$T_{total} = \frac{1}{2} m\dot{V}^2$$

$$= \frac{1}{2}.\rho.area.\dot{V}^2 \qquad (24)$$

After substituting (Eq. 22) and (Eq. 23) into (Eq. 24), finally obtaining the total kinetic energy (T_{total}):

$$T_{total} = \frac{\rho.ka_i^2}{4E'^2}\left[\frac{a_o}{\sqrt{2}}.\frac{w.\tau_o^2.\sin(wt)}{4\left[\sigma^2+\left(\tau_o.\sin\left(\frac{wt}{2}\right)\right)^2\right]^{1/2}}+\frac{1}{\sqrt{2}}\left[\sigma^2+\left(\tau_o.\sin\left(\frac{wt}{2}\right)\right)^2\right]^{\frac{1}{2}}.\frac{da}{dt}\right]^2 \qquad (25)$$

When the crack first started to expand, the value of the excess energy was converted into the total kinetic energy (U = T_{total}). when the excess energy rate was calculated using (Eq. 18), this was when the crack started to grow at an increased rate.

$$\left(\frac{\sigma^2}{2E}+\frac{2(1+v)}{E}\left(\tau_o.\sin\frac{wt}{2}\right)^2\right)\frac{\pi}{4}(a_i-a_o)^2=\frac{\rho.ka_i^2}{4E^2}*$$

$$\left[\frac{a_o}{\sqrt{2}}.\frac{w.\tau_o^2.\sin(wt)}{4\left[\sigma^2+\left(\tau_o.\sin\left(\frac{wt}{2}\right)\right)^2\right]^{1/2}}+\frac{1}{\sqrt{2}}\left[\sigma^2+\left(\tau_o.\sin\left(\frac{wt}{2}\right)\right)^2\right]^{1/2}.\frac{da}{dt}\right]^2 \qquad (26)$$

The equation for crack growth, model No. 2, that is used to estimate the rate of crack propagation at any moment after the fracture's beginning with the elastic limit. Both of these mathematical models have made use of the equivalent stress intensity factor, denoted by the letter (K_{equ}). This notation represents the difference between the highest possible value and the lowest possible value of the stress intensity factor. The value for constant tension stress 48.8 M Pa was determined for both specimens when the length of the crack was held constant at 5 mm. The greatest amount of shear cycling was applied to 6061 AA at 49.08 M Pa and to 5052 AA at 48.06 M Pa. This is the point at which the shear stress was at its lowest possible value of zero. A criteria of the maximum stress that used for mixed modes of loads when value ($K_{II} > 0$) from the references [24-25] was utilized in the calculations of this research to locate the crack direction theoretically. Where the values of K_I and K_{II} are calculated for each sample, and the sum of the values is entered into (Eq. 27) to find the direction of the inclination of the crack. The principle depends on the stresses surrounding and affecting the crack, and the ratios of their intensities to each other are what control the amount of inclination of the crack angle. this was done by using the mixed mode of loads [27].

$$\theta_c = \tan^{-1}\left(0.25 * \frac{KI}{KII} - \frac{1}{4}\sqrt{\left(\frac{KI}{KII}\right)^2 + 8}\right) \quad (\text{At } K_{II} > 0) \qquad (27)$$

3. Numerical Simulation

There are many programs for analysing fracture mechanics that can be adopted to predict the occurrence of failure and calculate the rate of crack growth, such as ANSYS, and ABAQUS [28-30]. These programs use different techniques and methods for calculating. In this research, the mechanical ANSYS version 2021.R1 was used. The simulation stages included drawing samples using mechanical APDL with dimensions 160 x 40 x 2 mm and a crack at the edge 5 mm in a straight specimen.

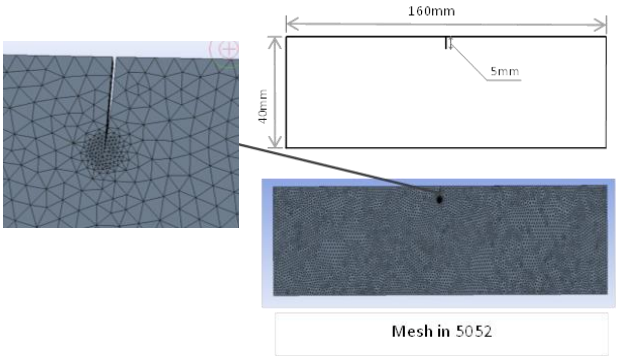

Figure 7. Dimensions and mesh for alloys

The work in the program consisted of three parts: the first part included drawing in the ANSYS program, entering the dimensions and shape of the sample, and choosing the types of sample materials to be tested. The second part to direct the program in determining the data related to the variables and the quality of the prediction is crack and loads on the sample, where the number of elements is 116135 and from the mesh list, a sphere with a radius of 1.2 mm is created at the edge of the crack and generate the mesh through it with a size of 0.2 mm , while the size of the rest of the mesh elements is 2 mm, so that the mesh is smaller in size and to obtain more accurate values. The type of elements used in this study on the plate is tetrahedral for all sizes of mesh elements.

From the last static structure, the boundary conditions was entered, so that Fixed Support was selected for the parts where the sample was installed, as well as instructing the remote displacement to apply a cyclic shear load of 0.00188 mm and instructing the pressure to apply the tensile load to the face to be applied. while the third part of the work involved finding the results using the Smart Crack Growth method that was used to analyse crack growth from a fracture list by selecting a pre-crack type and specifying the properties of the material that was entered in the program library, as well as the type of fatigue selection in the crack growth option, as well as specifying the Law of Paris in using it as a measure of fatigue. as shown in Fig. 7.

4. Results and discussion

In this part of the investigation, the results that were obtained analytically from the mathematical equations that were derived for samples of thin

aluminium alloys with a thickness of 2 mm and dimensions of 160 x 40 mm were discussed, where the table. 1 is shown the mechanical properties that used in the study. Additionally, a crack was made at the edge at an angle of 90 degrees with a length of 5 mm,

Table 1. Mechanical properties for alloys

Mechanical Properties	6061 AA	5052 AA
Ultimate stress (N/mm^2)	288.95	215.34
Yield stress (N/mm^2)	249.65	106.23
Elongation %	13.8	18.8
Hardening Vickers test	98	60
Elastic modules (Gpa)	68.9	70.3

and periodic loads were applied In-plane. As can be seen in Fig. 5, a constant tension was applied in the direction of the sample's longitudinal axis, while a periodic shear load was applied in the direction of the crack's parallel axis. Given that the number of cycles N is related to the amount of time necessary for growth (t), where the number of cycles N was discovered by the time required for growth by constant value every 1000 cycles equals 1 minute (This ratio between the number of revolutions and the time was determined based on separated study on an apparatus experimental that applied same loads in this study, and the number of revolutions was used with a capacity of 1000 revolutions per minute), the continuous crack growth in the sample by Increasing the crack length (a), the results shown in Fig. 8 and Fig. 9. Analytical testing confirmed that the initial fracture occurred at a cycle count of 250,000 for sample 6061 and 100,000 for sample 5052, respectively. In addition, the rate of fracture propagation in sample 6061 was discovered to be lower than that of sample 5052 through the body in the study that was conducted. It was also discovered that The rate of crack growth showed a value (0.000194, 0.000222) for sample 6061 in the first and second theoretical models, respectively, while the rate of growth in the analytical ANSYS program was (0.000208) in units of mm / sec.

While the rate of crack growth over time showed a speed (0.00056034, 0.000633) for sample 5052 in the first and second theoretical models, respectively, while the rate of growth in the analytical ANSYS program was (0.000666) in units of mm / sec.

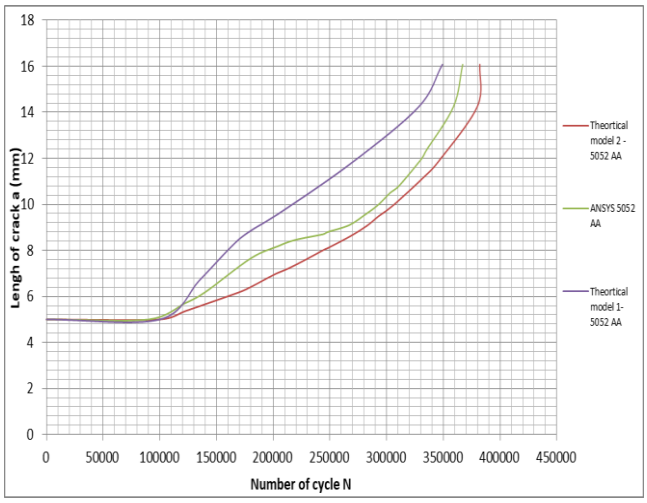

Figure 8. Length of crack vs. number of cycle N for alloy 5052

It has been noticed from Figs. 8 and 9 that there is a difference in the growth rate between the two sports models, as the first sports model gave more speed than the second sports model. Here it must be mentioned that when deriving the mathematical equations, the same equation for excess energy was relied upon to calculate the two mathematical models, but the difference is in the method of finding the kinetic energy, and this means that the amount given by the kinetic energy was greater in the first mathematical model than in the second, in order to calculate each displacement individually for each mode.

It was founded that the m and C values of the Paris equation derived analytically using the log plot approach both theoretically (model no.1,model no. 2), These results are specific to the values of the constants of the Paris equation, where, after plotting the results of the relationship between the change in crack length and the change in the number of cycles with the values of the change in the equivalent stress-intensity factor, those values were found for the two models, which are considered values in the case of multi-axial load. where the value of C is ($1.5849*10^{-6}$, $6.309*10^{-7}$) (mm/cycle)/(MPa$\sqrt{m}$) & m is (3, 2.428), respectively was found for alloy 6061, while the value of C is ($2.678*10^{-6}$, $4.6773*10^{-6}$) (mm/cycle)/(MPa$\sqrt{m}$) & m is (2.8321, 1.6609), respectively was found for alloy 5052.

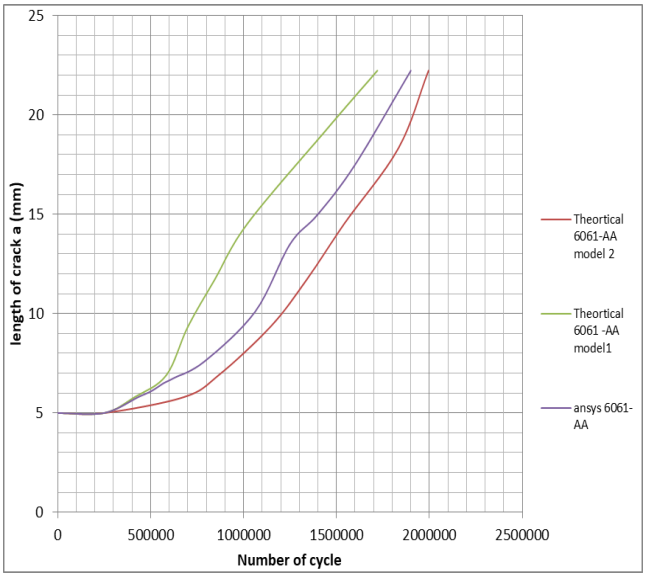

Figure 9. Length of crack vs. number of cycle N for alloy 6061

The crack in sample 5052 theoretically had a length of 16 mm, but the numerical analysis results were 18 mm, and the crack in sample 6061 theoretically had a length of 22 mm, but the numerical analysis results were 23 mm, indicating a convergence in the results for the second phase study. In Figures 8 and 9, the change ratios da and dN for the incision at length (14.5, 18) mm for samples 5052 and 6061 became closer in slope to 90 degrees, as shown in Figs. (8-9), indicating that it entered another stage in the crack growth propagate ratio at increasing the velocity of the crack.

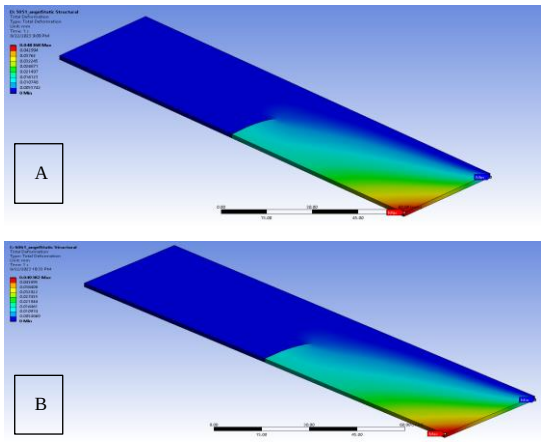

Figure 10. Total deflection for samples: A. 5052; B. 6061 in ANSYS.

In Fig. 10 shows the values of the location of higher deflections in samples 6061 and 5052.

Where the first and second mathematical models presented. The angle of trace for alloy 5052 is (24.896°), and the angle of trace for alloy 6061 is (30.1°), and the software shows that the angle of trace is (17.17°, 16.99°) for alloys 5052 and 6061, respectively see Fig. 11 and Fig. 12

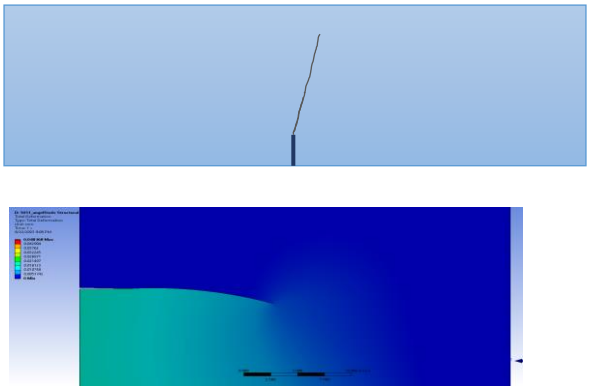

Figure 11. Directions sample 5052 theoretically and ANSYS

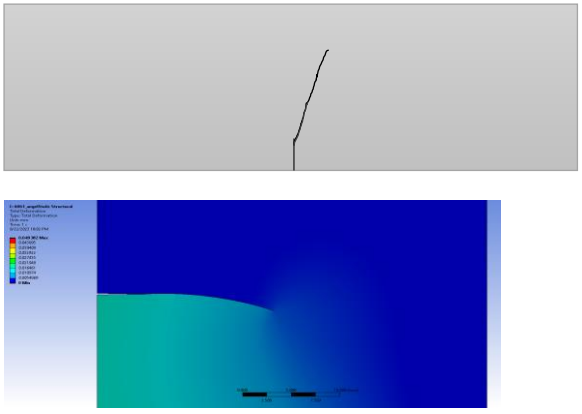

Figure 12. Directions sample 6061 theoretically and ANSYS.

When observing the results of the direction of the cracks shown in the study, the difference between the results of the direction can be attributed to the difference in the way of understanding the components and properties of the material and the effect of the homogeneity of its components in that study.

5. Conclusions

- Using Griffith's theory of crack development for thin plates, two mathematical models were developed in order to discover the crack propagation rate and compare the resultant rates with those produced by the analytical ANSYS software.
- It takes a longer amount of time for a crack to grow and approach the stage of fracture in aluminium sample 6061 than it does in sample 5052.
- The error percentage in crack growth rate in the sample 5052 for the theoretical model 1 and model 2 relative to the ANSYS program is found (15.1%, 4.09%), respectively
- The error percentage in crack growth rate in the sample 6061 for the theoretical model 1 and model 2 relative to the ANSYS program is found (6.73%, 5.4%), respectively
- The constants of the Paris equation gave good results for the values of C and m that were calculated in mixed mode by the effect of multi-axial fatigue loads.
- The amount of kinetic energy that was calculated for the separate modes gave higher values than that calculated in the case of the mixed mode.

Authors' contribution

All authors contributed equally to the preparation of this article.

Declaration of competing interest

The authors declare no conflicts of interest.

Orcid

Israa A. Mosleh: https://orcid.org/0009-0009-6304-2877

Fathi A. A. Alshamma : https://orcid.org/0000-0002-7670-5918

Funding source

This study didn't receive any specific funds.

Acknowledgements

We thank the Mechanical Department at Baghdad University for providing us with the resources and assistance that needed to finish this project. Finally, it appreciates all research participants' time and willingness to share their experiences. Their contributions have been crucial to our understanding and conclusions.

REFERENCES

[1] J. Toribio, J.-C. Matos, and B. González, "Paris Law-Based Approach to Fatigue Crack Growth in Notched Plates under Tension Loading," *Procedia Struct. Integr.*, vol. 5, pp. 1299–1303, 2017, doi: https://doi.org/10.1016/j.prostr.2017.07.115.

[2] Y. Li, H. Wang, and D. Gong, "The interrelation of the parameters in the Paris equation of fatigue crack growth," *Eng. Fract. Mech.*, vol. 96, pp. 500–509, 2012, doi: https://doi.org/10.1016/j.engfracmech.2012.08.016.

[3] K. Tanaka and S. Matsuoka, "A tentative explanation for two parameters, C and m, in Paris equation of fatigue crack growth," *Int. J. Fract.*, vol. 13, pp. 563–583,

1977.

[4] F. A. Alshamma and B. A. Ahmed, “Strain Analysis of Surface Cracked Thin Flat Plate under Cycling Impact Loading Effect,” *J. Eng.*, vol. 21, no. 4 SE-Articles, pp. 138–157, Dec. 2015, [Online]. Available: https://joe.uobaghdad.edu.iq/index.php/main/article/view/44

[5] H. H. Jasim, “Evaluation of Fatigue Behavior of Epoxy Coatings used for Potable Water Storage Tanks,” *J. Eng.*, vol. 26, no. 3 SE-Articles, pp. 18–32, Mar. 2020, doi: 10.31026/j.eng.2020.03.02.

[6] B. V Kopei, O. I. Zvirko, T. P. Venhrynyuk, Z. V Slobodyan, and I. P. Shtoiko, “Elevation of the Fatigue Strength of Pump Rods as a Result of Treatment with a Special Medium,” *Mater. Sci.*, vol. 56, no. 1, pp. 125–131, 2020, doi: 10.1007/s11003-020-00406-0.

[7] M. A. A. Al- Jaafari, “Heat Treatments Effects on the Fatigue Behaviors of Aluminum Nano-Composite Alloys,” *Iraqi J. Sci.*, vol. 62, no. 11 SE-Physics, pp. 4397–4405, Dec. 2021, doi: 10.24996/ijs.2021.62.11(SI).20.

[8] R. Ibrahim Mhawes, “Study The Effect of Multi Axial Cycling Loading on The Dynamic Crack Propagation In Aluminum Plates,” *Int. J. Mech. Eng.*, vol. 7, pp. 305–313, 2022.

[9] A. D. Assi, “Influence of Al2O3 Nanoparticles Addition to AA6082-T6 on Mechanical Properties by Stir Casting Technique,” *IOP Conf. Ser. Mater. Sci. Eng.*, vol. 881, no. 1, p. 12081, 2020, doi: 10.1088/1757-899X/881/1/012081.

[10] L. Ewalds , H and H. Wanhill , R , J, *FRACTURE MECHANICS*, FOURTH. LONDON: Edwrd Arnold, 1989.

[11] H. Tada, H. A. Ernst, and P. C. Paris, “Westergaard stress functions for displacement-prescribed crack problems—I,” *Int. J. Fract.*, vol. 61, no. 1, pp. 39–53, 1993, doi: 10.1007/BF00032338.

[12] C. T. Sun and Z.-H. Jin, “The Elastic Stress Field around a Crack Tip,” 2012, pp. 25–75. doi: 10.1016/B978-0-12-385001-0.00003-1.

[13] W. Thein, “Stress intensity factors determined by use of westergaard’s stress functions,” *Eng. Fract. Mech.*, vol. 20, no. 1, pp. 65–73, 1984, doi: https://doi.org/10.1016/0013-7944(84)90115-2.

[14] J. knot, *fundamentals of fracture mechanics*, FIRST. LONDON, 1973.

[15] H. M. Hasoon, “Modified decomposition method for solving linear FredholmVolterra integral equations,” *IOSR J. Math.*, vol. 12, no. 2, pp. 159–160, 2016, [Online]. Available: https://www.iosrjournals.org/iosr-jm/papers/Vol12-issue2/Version-1/R01221159160.pdf

[16] H. Tada, H. A. Ernst, and P. C. Paris, “Westergaard stress functions for displacement-prescribed cracks-II. Extension to mixed problems,” *Int. J. Fract.*, vol. 67, pp. 151–167, 1994, [Online]. Available: https://api.semanticscholar.org/CorpusID:122965587

[17] H. Al-Quraishi, M. J. Lafta, and A. A. Abdulridha, “Direct Shear Behavior of Fiber Reinforced Concrete Elements,” *J. Eng.*, vol. 24, no. 1 SE-Articles, pp. 231–248, Jan. 2018, doi: 10.31026/j.eng.2018.01.16.

[18] M. Y. Eisa, B. A. Abdulmajeed, and C. K. Hawee, “Kinetic Study of the Leaching of Iraqi Akashat Phosphate Ore Using Lactic Acid,” *Al-Khwarizmi Eng. J.*, vol. 14, no. 1 SE-Articles, pp. 128–135, Apr. 2018, doi: 10.22153/kej.2018.08.006.

[19] F. Barras, M. Aldam, T. Roch, E. A. Brener, E. Bouchbinder, and J.-F. Molinari, “The emergence of crack-like behavior of frictional rupture: Edge singularity and energy balance,” *Earth Planet. Sci. Lett.*, vol. 531, p. 115978, 2020, doi: https://doi.org/10.1016/j.epsl.2019.115978.

[20] H. P. Stüwe and R. Pippan, “On the energy balance of fatigue crack growth,” *Comput. Struct.*, vol. 44, no. 1, pp. 13–17, 1992, doi: https://doi.org/10.1016/0045-7949(92)90218-O.

[21] S. E. A. B. Abdel-Rahman A. Ragab, *Engineering Solid Mechanics*, Fist. Boca Raton: 20 December 2019, 1998. doi: https://doi.org/10.1201/9780203757307.

[22] K. Sadananda, K. N. Solanki, and A. K. Vasudevan, “Subcritical crack growth and crack tip driving forces in relation to material resistance,” vol. 35, no. 4–5, pp. 251–265, 2017, doi: doi:10.1515/corrrev-2017-0034.

[23] F. M. Mohammed, “Mechanical Properties Investigation of Composite Material Under Different Parameters Variations,” *Al-Khwarizmi Eng. J.*, vol. 13, no. 1 SE-Articles, pp. 74–83, Mar. 2017, doi: 10.22153/kej.2017.09.001.

[24] M. Maksimović, I. Vasović, K. Maksimović, S. Maksimović, and D. Stamenković, “Crack growth analysis and residual life estimation of structural elements under mixed modes,” *Procedia Struct. Integr.*, vol. 13, pp. 1888–1894, 2018, doi: https://doi.org/10.1016/j.prostr.2018.12.324.

[25] Z. A. Alkaissi and D. A. Al Khafagy, “Propagation Mechanisms for Surface Initiated Cracking in Composite Pavements,” *Al-Khwarizmi Eng. J.*, vol. 5, no. 3 SE-Articles, pp. 51–59, Sep. 2009, [Online]. Available: https://alkej.uobaghdad.edu.iq/index.php/alkej/article/view/571

[26] M. H. Aliabadi, “3.02 - Boundary Element Methods in Linear Elastic Fracture Mechanics,” I. Milne, R. O. Ritchie, and B. B. T.-C. S. I. Karihaloo, Eds., Oxford: Pergamon, 2003, pp. 89–125. doi: https://doi.org/10.1016/B0-08-043749-4/03068-8.

[27] Y. A. Fageehi and A. M. Alshoaibi, “Numerical Simulation of Mixed-Mode Fatigue Crack Growth for Compact Tension Shear Specimen,” Adv. Mater. Sci. Eng., vol. 2020, p. 5426831, 2020, doi: 10.1155/2020/5426831.

[28] Fahem, A., A. Alshamma, F. (2009). 'A study of the effect of impact loading on dsifs and crack propagation in plate', Al-Qadisiyah Journal for Engineering Sciences, 2(2), pp. 288-303. https://doi.org/10.30772/qjes.2009.34785

[29] Piyush Singhal, Ch. Srividhya, Ashwani Kumar, Shilpi Chauhan, Zahraa N. Salman, Alok Jain, "Modelling and Simulation of Fracture Mechanics and Failure Analysis of Materials using FEA", E3S Web Conf. 430 01113 (2023). DOI: 10.1051/e3sconf/202343001113

[30] Ali Fahem, Addis Kidane, Michael A. Sutton, "Geometry factors for Mode I stress intensity factor of a cylindrical specimen with spiral crack subjected to torsion", Engineering Fracture Mechanics, Volume 214, 2019, Pages 79-94, ISSN 0013-7944, https://doi.org/10.1016/j.engfracmech.2019.04.007.